
Evaluating Adversarial Attacks on ImageNet: A Reality Check on Misclassification Classes

Utku Ozbulak*

Ghent University, Belgium
utku.ozbulak@ugent.be

Maura Pintor*

University of Cagliari, Italy
maura.pintor@unica.it

Arnout Van Messem

University of Liège, Belgium
Arnout.vanmessem@uliege.be

Wesley De Neve

Ghent University, Belgium
wesley.deneve@ugent.be

Abstract

Although ImageNet was initially proposed as a dataset for performance benchmarking in the domain of computer vision, it also enabled a variety of other research efforts. Adversarial machine learning is one such research effort, employing deceptive inputs to fool models in making wrong predictions. To evaluate attacks and defenses in the field of adversarial machine learning, ImageNet remains one of the most frequently used datasets. However, a topic that is yet to be investigated is the nature of the classes into which adversarial examples are misclassified. In this paper, we perform a detailed analysis of these misclassification classes, leveraging the ImageNet class hierarchy and measuring the relative positions of the aforementioned type of classes in the unperturbed origins of the adversarial examples. We find that 71% of the adversarial examples that achieve model-to-model adversarial transferability are misclassified into one of the top-5 classes predicted for the underlying source images. We also find that a large subset of untargeted misclassifications are, in fact, misclassifications into semantically similar classes. Based on these findings, we discuss the need to take into account the ImageNet class hierarchy when evaluating untargeted adversarial successes. Furthermore, we advocate for future research efforts to incorporate categorical information.

1 Introduction

Soon after its release, ImageNet [31] became the de facto standard dataset for performance benchmarking in the field of computer vision, primarily thanks to the diverse set of images and classes it contains. This diversity allowed for research on various vision tasks, including, but not limited to, classification [20, 36], segmentation [1, 23], and localization [14, 30]. Although the tasks put forward during the introduction of ImageNet were considered to be some of the hardest problems to address in the field of computer vision, a number of deep neural networks (DNNs) were, in recent years, able to achieve super-human results on many of these challenges, thus effectively “solving” the aforementioned problems [9]. However, research efforts that make use of ImageNet are not limited to the performance-oriented tasks mentioned before. Indeed, thanks to the diverse set of images it contains, ImageNet enabled a large number of research efforts beyond its initial scope, allowing researchers to experiment with model interpretability [34, 37], model calibration [12], object relations [32], fairness [42], and many other topics.

One research field that was enriched by the availability of ImageNet is the field of study that focuses on adversarial examples. In this context, the term “adversarial examples” refers to meticulously

*Equal contribution.

created data points that come with a malicious intent, aimed at deceiving models that are performing a pre-defined task, steering the prediction outcome in favor of the adversary [2, 40]. Although adversarial examples are a threat for predictive models in domains other than the domain of computer vision [3, 28], the latter is acknowledged to be the one that suffers the most from adversarial examples, since an adversarial example created from a genuine image, through the use of adversarial perturbation, often looks the same as its unperturbed counterpart [10, 25]. This makes it, in most cases, impossible to detect adversarial examples by visually inspecting images.

Although the vulnerability of DNNs to adversarial examples in the image domain was originally mostly evaluated through the usage of two datasets, namely MNIST [22] and CIFAR [19], the authors of [4] revealed that methods derived through the usage of one of these datasets do not necessarily generalize to other datasets. In particular, compared to ImageNet, both of the aforementioned datasets contain images with a smaller resolution and a lower number of classes. As a result, most of the research efforts in recent years started to favor ImageNet over MNIST and CIFAR [7, 11, 39, 41].

From the perspective of adversarial evaluation, ImageNet does not only allow for most, if not all, of the research work that was performed using the previously mentioned datasets, it also enables a wide range of additional research topics in the area of adversariality, such as investigations with regards to regional perturbation [18], color channels [35, 41], and defenses that use certain properties of natural images [13]. However, as demonstrated in this paper, ImageNet has a major shortcoming when it comes to evaluating adversarial attacks, especially in model-to-model transferability scenarios: a large number of synsets/classes in ImageNet are semantically highly similar to one another.

Different from previous research efforts that mostly focus on generating more effective adversarial perturbations or evaluating adversarial defenses, we investigate a topic that is yet to be touched upon: untargeted misclassification classes for adversarial examples. Specifically, with the help of two of the most frequently used adversarial attacks and seven unique DNN architectures, including two recently proposed vision transformer architectures, we present a large-scale study that solely focuses on model-to-model adversarial transferability and misclassification classes in the context of ImageNet, resulting in the following contributions:

- In model-to-model transferability scenarios, we demonstrate that a large portion of adversarial examples are classified into the top-5 predictions obtained for their source image counterparts.
- With the help of the ImageNet class hierarchy, we show that adversarial examples created from certain synset collections are mostly misclassified into classes belonging to the same collections (e.g., a dog breed is misclassified as another dog breed).
- Interestingly, we can make the two aforementioned observations consistently for all of the evaluated models, as well as for both adversarial attacks. As a result, we discuss the necessity of evaluating misclassification classes when experimenting with adversarial attacks and untargeted misclassification in the context of ImageNet.

2 Adversarial attacks

Given an M -class classification problem, a data point $\mathbf{x} \in \mathbb{R}^k$ and its categorical association $\mathbf{y} \in \mathbb{R}^M$ associated with a correct class k ($y_k = 1$ and $y_m = 0, \forall m \in \{0, \dots, M\} \setminus \{k\}$) are used to train a machine learning model represented by θ . Let $g(\theta, \mathbf{x}) \in \mathbb{R}^M$ represent the prediction (logit) produced by the model θ and a data point \mathbf{x} . This data point is then assigned to the class that contains the largest output value $G(\theta, \mathbf{x}) = \arg \max(g(\theta, \mathbf{x}))$. When $G(\theta, \mathbf{x}) = \arg \max(\mathbf{y})$, this prediction is recognized as the correct one. For the given setting, a perturbation Δ bounded by an L_p ball centered at \mathbf{x} with radius ϵ is said to be an *adversarial perturbation* if $G(\theta, \mathbf{x}) \neq G(\theta, \mathbf{x} + \Delta)$. In this case, $\hat{\mathbf{x}} = \mathbf{x} + \Delta$ is said to be an *adversarial example*.

Adversarial examples can be highly *transferable*: an adversarial sample that fools a certain classifier can also fool completely different classifiers that have been trained for the same task [6, 8, 29]. This property, which is called transferability of adversarial examples, is a popular metric for assessing the effectiveness of a particular attack. Let θ_1 and θ_2 represent two DNNs and let \mathbf{x} , k , and $\hat{\mathbf{x}}_1$ be a genuine image, the correct class of this image, and a corresponding adversarial example, respectively, with the adversarial example generated from this genuine image using an attack that targets a class c by leveraging the DNN represented by θ_1 . If $G(\theta_1, \hat{\mathbf{x}}_1) = G(\theta_2, \hat{\mathbf{x}}_1) = c$ and $G(\theta_{\{1,2\}}, \mathbf{x}) = k$, then the adversarial example is said to have achieved *targeted adversarial transferability* to the model θ_2 . If $G(\theta_1, \hat{\mathbf{x}}_1) = c$ but $G(\theta_2, \hat{\mathbf{x}}_1) \notin \{c, k\}$, the adversarial example in question is classified into a class

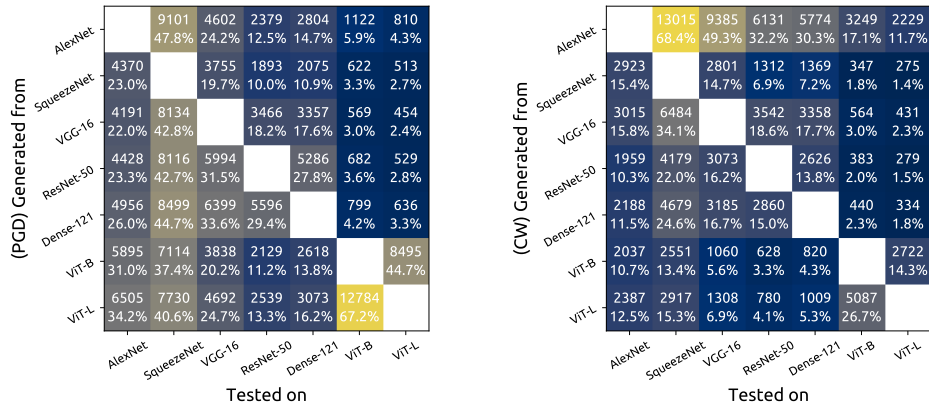


Figure 1: Number (percentage) of source images that became adversarial examples with PGD (*left*) and CW (*right*). Adversarial examples are generated by the models listed along the y -axis and tested by the models listed along the x -axis.

that is different than the targeted one (c) and the correct one (k). In cases like this, an adversarial example is said to have achieved *untargeted adversarial* transferability.

In the context of ImageNet, the success of targeted transferability for adversarial examples is known to be abysmally lower compared to the success of untargeted transferability [38]. As a result, many studies that propose a novel attack or perform a large-scale analysis of model-to-model transferability use untargeted transferability when showcasing the effectiveness of attacks, without evaluating the classes that adversarial examples are classified into [7, 11, 41]. Therefore, in this work, we investigate the success of untargeted adversarial transferability and the characteristics of misclassification classes.

3 Methodology

Models – In order to evaluate a variety of model-to-model adversarial transferability scenarios, we employ the following architectures: AlexNet [20], SqueezeNet [17], VGG-16 [36], ResNet-50 [15], and DenseNet-121 [16], as well as two recently proposed vision transformer architectures, namely ViT-Base/16 – 224 and ViT-Large/16 – 224 [9].

Data – For our adversarial attacks (see further in this section), we use images from the ImageNet validation set as inputs. Hereafter, these unperturbed input images will be referred to as *source images*. In order to perform a trustworthy analysis of adversarial transferability, we ensure that all source images are correctly classified by all employed models. To that end, we filter out all images incorrectly classified by at least one model, leaving us with 19,025 source images to work with.

ImageNet hierarchy – Classes in ImageNet are organized according to the WordNet hierarchy [26, 31], grouping classes into various collections depending on their semantic meaning. We use the aforementioned hierarchy in order to measure intra-collection adversarial misclassifications. In that respect, an intra-collection misclassification is when an adversarial example created from a source image that belongs to a class under a collection is misclassified into a class under the same collection (e.g., an image belonging to a cat breed misclassified as another breed of cat is an intra-collection misclassification for the *Feline* collection). More details about the ImageNet hierarchy are given in the supplementary material (see Figure I).

Attacks – We use the adversarial examples generated for our previous study [27], where those adversarial examples are generated using two of the most commonly used attacks: Projected Gradient Descent (PGD) [24] and Carlini & Wagner’s attack (CW) [5].

PGD can be seen as a generalization of L_∞ attacks [10, 21], aiming at finding an adversarial example \hat{x} that satisfies $\|\hat{x} - x\|_\infty < \epsilon$. The adversarial example is iteratively generated as follows:

$$\hat{x}^{(n+1)} = \Pi_\epsilon \left(\hat{x}^{(n)} - \alpha \text{sign}(\nabla_x J(g(\theta, \hat{x}^{(n)}))_c) \right), \quad (1)$$

with $\hat{x}^{(1)} = x$, c the selected class, and $J(\cdot)$ the cross-entropy loss. We use PGD with 50 iterations and set ϵ to $38/255$. We adopt this constraint as the maximum perturbation-size bound in order to be able to produce a large number of adversarial examples that achieve model-to-model transferability.

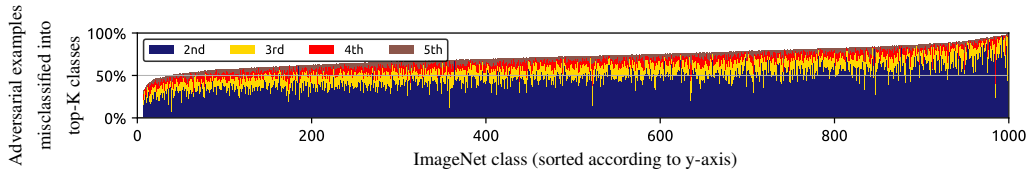


Figure 2: Number of adversarial examples, given per class, that are classified into the top- $\{2, 3, 4, 5\}$ classes predicted for their underlying source images.

CW, on the other hand, is a complex attack that incorporates L_2 norm minimization:

$$\text{mimize } \|\mathbf{x} - (\mathbf{x} + \Delta)\|_2^2 + f(\mathbf{x} + \Delta). \quad (2)$$

In the paper introducing CW [5], multiple loss functions (i.e., f) are discussed. However, in later works, the creators of CW prefer to make use of the loss function that is constructed as follows:

$$f(\mathbf{x}) = \max(\max\{g(\theta, \mathbf{x})_i : i \neq c\} - g(\theta, \mathbf{x})_c, -\kappa), \quad (3)$$

where this loss compares the predicted logit value of target class c with the predicted logit value of the next-most-likely class i . The constant κ can be used to adjust the *strength* of the produced adversarial examples (for our experiments, we use $\kappa = 20$ and the settings described in [5] and [27]).

We keep executing the attacks until a source image becomes an adversarial example or until the attacks reach a maximum number of iterations. At each iteration, we examine whether or not the images under consideration became adversarial examples for the aforementioned models.

4 Experiments

Leveraging the attacks described above and through the usage of 19,025 source images that are correctly classified by the models employed, we create 289,244 adversarial examples, where 173,549 of those adversarial examples are generated with PGD and 115,695 with CW. Detailed untargeted model-to-model transferability successes of those adversarial examples can be found in Figure 1.

To investigate misclassifications made into semantically similar classes, we first have a look at the adversarial examples that are misclassified into classes that lie in the top-5 positions of their source image predictions, where the four remaining classes, apart from the first one, are the classes that were deemed to be the most-likely prediction classes by the model under consideration, with the first one being the correct classification. Doing so, we provide Figure 2, with this figure displaying, for each class, the percentage of adversarial examples that had their predictions changed into one of the top-5 classes as described above. Specifically, we observe that 215,717 (approximately 71%) adversarial examples are predicted into one of the top-5 predictions of their unperturbed source images, where these classes in the top-5 are often highly similar to the correct predictions for the source images the adversarial examples are generated from (see Figure II in the supplementary material).

Although this graph hints that a large portion of untargeted adversarial transferability successes are (plausible) misclassifications rather than adversarial successes, on its own, it does not provide enough evidence to make such a claim. In order to solidify this observation, we expand on misclassifications and utilize the ImageNet class hierarchy. In Table 1, we provide the count and the percentage of adversarial examples that are originating from a number of collections and their intra-collection misclassification rates for a number of collections under the *Organism* branch of the hierarchy. Table 1 represents the aforementioned measurements for all adversarial examples that achieved adversarial transferability to any of the models and with any attack.

Naturally, the larger the collection, the higher the intra-collection misclassification rate will be. For example, a source image taken from the *Organism* collection has 409 other classes that may contribute to intra-collection misclassification. However, even for smaller, more granular collections such as the *Bird* collection, which only contains 59 classes, we observe that adversarial examples are more-often-than-not misclassified into the classes in the same collection. Furthermore, a number of collections such as *Canine*, *Bird*, *Reptilian*, and *Arthropod* stand out among other collections for having remarkably high intra-collection misclassification rates. For example, 84% of all adversarial examples that originate from a canine (i.e., dog) image are misclassified as another breed of canine.

Table 1: For the adversarial examples that achieved model-to-model transferability, intra-collection misclassifications and misclassifications into the top- $\{3,5\}$ prediction classes in the target models are provided. The results for the adversarial examples are grouped into collections according to the classes of their source image origins.

Hierarchy	Collection	Classes in collection	Source images in collection	Adversarial examples originating from collection	Intra-collection misclassifications		Misclassification into top-K classes	
					Count	%	Top-3	Top-5
	All	1000	19,025	289,244	289,244	100.0%	59.6%	71.1%
1	Organism	410	9,390	147,621	132,865	90.0%	61.2%	72.8%
1.1	Creature	398	9,009	143,996	130,409	90.6%	61.4%	73.1%
1.1.1	Domesticated animal	123	2,316	50,036	41,978	83.9%	63.4%	75.6%
1.1.2	Vertebrate	337	7,692	126,913	112,828	88.9%	61.3%	73.2%
1.1.2.1	Mammalian	218	4,665	89,004	76,351	85.8%	61.4%	73.5%
1.1.2.1.1	Primate	20	475	9,333	5,301	56.8%	58.9%	70.4%
1.1.2.1.2	Hoofed mammal	17	419	6,206	2,751	44.3%	58.4%	71.6%
1.1.2.1.3	Feline	13	319	3,895	1,998	51.3%	64.3%	75.9%
1.1.2.1.4	Canine	130	2,502	53,294	45,089	84.6%	63.5%	75.7%
1.1.2.2	Aquatic vertebrate	16	366	5,355	2,383	44.5%	65.0%	75.6%
1.1.2.3	Bird	59	1,937	22,402	15,993	71.4%	59.8%	71.3%
1.1.2.4	Reptilian	36	547	7,635	4,795	62.8%	63.8%	75.2%
1.1.2.4.1	Saurian	11	188	2,416	1,050	43.5%	58.4%	71.1%
1.1.2.4.2	Serpent	17	223	3,202	1,700	53.1%	67.0%	77.1%
1.1.3	Invertebrate	61	1,317	17,083	10,698	62.6%	61.9%	72.3%
1.1.3.1	Arthropod	47	1,018	13,200	8,863	67.1%	63.1%	73.5%
1.1.3.1.1	Insect	27	652	7,850	4,468	56.9%	59.9%	70.5%
1.1.3.1.2	Arachnoid	9	189	2,824	1,476	52.3%	69.7%	79.5%
1.1.3.1.3	Crustacean	9	137	2,035	955	46.9%	70.0%	80.1%

In Table 1, we also provide misclassifications into the top-3 and the top-5 classes for adversarial examples that are originating from source images taken from individual collections. As can be seen, the observations we made when evaluating all adversarial examples also hold true for individual collections, where most of the adversarial examples in those collections have a misclassification rate of about 60% and 70% for the top-3 and the top-5 classes, respectively. To make matters worse, we can even see trends similar to the aforementioned observations when we filter adversarial examples for individual attacks and when we investigate misclassifications on a model-to-model basis, demonstrating that our observations are not specific to a single model or to one of the attacks. Extended results covering more collections and individual models/attacks can be found in the supplementary material (Table I to Table V).

5 Conclusions and outlook

In the context of a classification problem, what differentiates an adversarial success from a plausible misclassification? If an adversarial example is misclassified into a class that is highly similar to the class of its unperturbed origin, should it still be considered an adversarial success? In this case, how should we measure the similarity between the classes? The aforementioned questions are not trivial to answer, and different answers may find different logical explanations depending on the context of the evaluation performed. However, given that the threat of adversarial examples is evaluated from the perspective of security, does a semantically similar misclassification that has been made in the context of ImageNet (e.g., a brown dog breed misclassified as another brown dog breed) carry the same weight as a lethal misclassification in the context of self-driving cars (e.g., a road sign misclassification leading to an accident)?

Finding answers to the questions presented above requires meticulous investigations on the topic of misclassification classes, where these investigations should involve various threat scenarios, similar to the work presented in [33, 43, 44]. In this paper, we took one of the first steps in analyzing misclassification classes in the context of ImageNet, with the help of large-scale experiments and the ImageNet class hierarchy, showing that a large number of untargeted adversarial misclassifications in model-to-model transferability scenarios are, in fact, plausible misclassifications. In particular, we observe that categories under the *Organism* branch have considerably high intra-collection misclassifications compared to classes in the *Artifact* branch. To aid future work on this topic in the context of ImageNet, we share an easy-to-use class hierarchy of ImageNet, as well as other resources, in the following repository: <https://github.com/utkuozbulak/imagenet-adversarial-image-evaluation>.

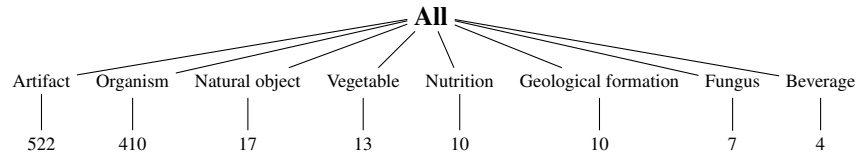
References

- [1] V. Badrinarayanan, A. Kendall, and R. Cipolla. Segnet: A Deep Convolutional Encoder-Decoder Architecture For Image Segmentation. *IEEE transactions on pattern analysis and machine intelligence*, 2017.
- [2] B. Biggio, I. Corona, D. Maiorca, B. Nelson, N. Šrndić, P. Laskov, G. Giacinto, and F. Roli. Evasion Attacks Against Machine Learning At Test Time. In *Joint European Conference on Machine Learning and Knowledge Discovery in Databases*, 2013.
- [3] N. Carlini and D. Wagner. Audio Adversarial Examples: Targeted Attacks on Speech-to-Text. In *2018 IEEE Security and Privacy Workshops (SPW)*. IEEE, 2018.
- [4] N. Carlini and D. A. Wagner. Adversarial Examples Are Not Easily Detected: Bypassing Ten Detection Methods. *Proceedings of the 10th ACM Workshop on Artificial Intelligence and Security*, 2017.
- [5] N. Carlini and D. A. Wagner. Towards Evaluating The Robustness of Neural Networks. *2017 IEEE Symposium on Security and Privacy*, 2017.
- [6] S. Cheng, Y. Dong, T. Pang, H. Su, and J. Zhu. Improving Black-box Adversarial Attacks with a Transfer-based Prior. In *Advances in Neural Information Processing Systems*, 2019.
- [7] F. Croce and M. Hein. Sparse and Imperceivable Adversarial Attacks. In *Proceedings of the IEEE International Conference on Computer Vision*, 2019.
- [8] A. Demontis, M. Melis, M. Pintor, M. Jagielski, B. Biggio, A. Oprea, C. Nita-Rotaru, and F. Roli. Why do adversarial attacks transfer? explaining transferability of evasion and poisoning attacks. In *28th USENIX Security Symposium (USENIX Security 19)*, pages 321–338, Santa Clara, CA, aug 2019. USENIX Association.
- [9] A. Dosovitskiy, L. Beyer, A. Kolesnikov, D. Weissenborn, X. Zhai, T. Unterthiner, M. Dehghani, M. Minderer, G. Heigold, S. Gelly, J. Uszkoreit, and N. Houlsby. An Image is Worth 16x16 Words: Transformers for Image Recognition at Scale. In *International Conference on Learning Representations*, 2021.
- [10] I. Goodfellow, J. Shlens, and C. Szegedy. Explaining and Harnessing Adversarial Examples. *International Conference on Learning Representations*, 2015.
- [11] C. Guo, J. R. Gardner, Y. You, A. G. Wilson, and K. Q. Weinberger. Simple Black-box Adversarial Attacks. *International Conference on Machine Learning*, 2019.
- [12] C. Guo, G. Pleiss, Y. Sun, and K. Q. Weinberger. On Calibration of Modern Neural Networks. In *International Conference on Machine Learning*, 2017.
- [13] C. Guo, M. Rana, M. Cisse, and L. Van Der Maaten. Countering Adversarial Images Using Input Transformations. *CoRR*, abs/1711.00117, 2017.
- [14] K. He, G. Gkioxari, P. Dollár, and R. Girshick. Mask R-CNN. In *Proceedings of the IEEE International Conference on Computer Vision*, 2017.
- [15] K. He, X. Zhang, S. Ren, and J. Sun. Deep Residual Learning For Image Recognition. In *Proceedings of the IEEE Conference on Computer Vision and Pattern Recognition*, 2016.
- [16] G. Huang, Z. Liu, L. Van Der Maaten, and K. Q. Weinberger. Densely Connected Convolutional Networks. In *Proceedings of the IEEE Conference on Computer Vision and Pattern Recognition*, 2017.
- [17] F. N. Iandola, S. Han, M. W. Moskewicz, K. Ashraf, W. J. Dally, and K. Keutzer. SqueezeNet: AlexNet-level Accuracy with 50x Fewer Parameters and < 0.5 MB Model Size. *CoRR*, abs/1602.07360, 2016.
- [18] D. Karmon, D. Zoran, and Y. Goldberg. Lavan: Localized and Visible Adversarial Noise. *International Conference on Machine Learning*, 2018.
- [19] A. Krizhevsky and G. Hinton. Learning Multiple Layers Of Features From Tiny Images. Technical report, Citeseer, 2009.
- [20] A. Krizhevsky, I. Sutskever, and G. E. Hinton. ImageNet Classification with Deep Convolutional Neural Networks. In *Advances in Neural Information Processing Systems*, 2012.
- [21] A. Kurakin, I. Goodfellow, and S. Bengio. Adversarial Examples In The Physical World. *Workshop Track, International Conference on Learning Representations*, 2016.

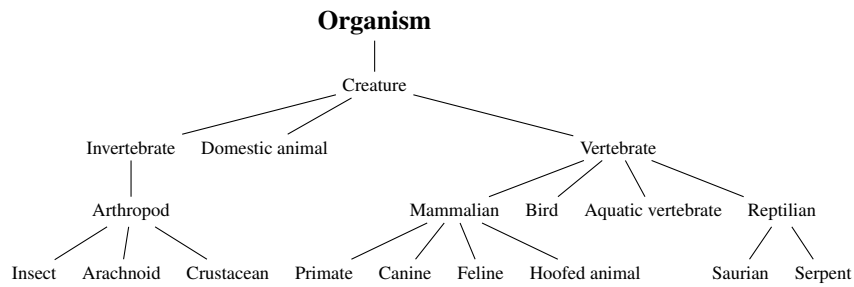
- [22] Y. LeCun, L. Bottou, Y. Bengio, and P. Haffner. Gradient-Based Learning Applied To Document Recognition. *Proceedings of the IEEE*, 1998.
- [23] J. Long, E. Shelhamer, and T. Darrell. Fully Convolutional Networks For Semantic Segmentation. In *Proceedings of the IEEE Conference on Computer Vision and Pattern Recognition*, 2015.
- [24] A. Madry, A. Makelov, L. Schmidt, D. Tsipras, and A. Vladu. Towards Deep Learning Models Resistant To Adversarial Attacks. *International Conference on Learning Representations*, 2018.
- [25] P. McDaniel, N. Papernot, and Z. B. Celik. Machine Learning In Adversarial Settings. *IEEE Security & Privacy*, 2016.
- [26] G. A. Miller. *WordNet: An electronic lexical database*. MIT press, 1998.
- [27] U. Ozbulak, E. T. Anzaku, W. D. Neve, and A. V. Messem. Selection of Source Images Heavily Influences the Effectiveness of Adversarial Attacks. *CoRR*, abs/2106.07141, 2021.
- [28] U. Ozbulak, B. Vandersmissen, A. Jalalvand, I. Couckuyt, A. Van Messem, and W. De Neve. Investigating the significance of adversarial attacks and their relation to interpretability for radar-based human activity recognition systems. *Computer Vision and Image Understanding*, 2021.
- [29] N. Papernot, P. D. McDaniel, and I. Goodfellow. Transferability In Machine Learning: From Phenomena To Black-Box Attacks Using Adversarial Samples. *CoRR*, abs/1605.07277, 2016.
- [30] S. Ren, K. He, R. Girshick, and J. Sun. Faster R-CNN: Towards Real-Time Object Detection with Region Proposal Networks. In *Advances in Neural Information Processing Systems*, 2015.
- [31] O. Russakovsky, J. Deng, H. Su, J. Krause, S. Satheesh, S. Ma, Z. Huang, A. Karpathy, A. Khosla, M. Bernstein, A. C. Berg, and L. Fei-Fei. ImageNet Large Scale Visual Recognition Challenge. *International Journal of Computer Vision*, 2015.
- [32] O. Russakovsky and L. Fei-Fei. Attribute Learning in Large-scale Datasets. In *European Conference of Computer Vision (ECCV), International Workshop on Parts and Attributes*, 2010.
- [33] L. Schwinn, R. Raab, A. Nguyen, D. Zanca, and B. Eskofier. Exploring Misclassifications of Robust Neural Networks to Enhance Adversarial Attacks. *CoRR*, abs/2105.10304, 2021.
- [34] R. R. Selvaraju, A. Das, R. Vedantam, M. Cogswell, D. Parikh, and D. Batra. Grad-Cam: Why Did You Say That? Visual Explanations From Deep Networks Via Gradient-Based Localization. *Proceedings of the IEEE Conference on Computer Vision and Pattern Recognition*, 2016.
- [35] A. S. Shamsabadi, R. Sanchez-Matilla, and A. Cavallaro. Colorfool: Semantic Adversarial Colorization. In *Proceedings of the IEEE Conference on Computer Vision and Pattern Recognition*, 2020.
- [36] K. Simonyan and A. Zisserman. Very Deep Convolutional Networks For Large-Scale Image Recognition. *International Conference on Learning Representations*, 2015.
- [37] J. T. Springenberg, A. Dosovitskiy, T. Brox, and M. Riedmiller. Striving For Simplicity: The All Convolutional Net. *CoRR*, abs/1412.6806, 2014.
- [38] D. Su, H. Zhang, H. Chen, J. Yi, P.-Y. Chen, and Y. Gao. Is Robustness the Cost of Accuracy?—A Comprehensive Study on the Robustness of 18 Deep Image Classification Models. In *Proceedings of the European Conference on Computer Vision*, 2018.
- [39] J. Su, D. V. Vargas, and K. Sakurai. Empirical Evaluation On Robustness Of Deep Convolutional Neural Networks Activation Functions Against Adversarial Perturbation. In *International Symposium on Computing and Networking Workshops (CANDARW)*. IEEE, 2018.
- [40] C. Szegedy, W. Zaremba, I. Sutskever, J. Bruna, D. Erhan, I. Goodfellow, and R. Fergus. Intriguing Properties Of Neural Networks. *International Conference on Learning Representations*, 2014.
- [41] K. Xu, S. Liu, P. Zhao, P.-Y. Chen, H. Zhang, Q. Fan, D. Erdogmus, Y. Wang, and X. Lin. Structured Adversarial Attack: Towards General Implementation and Better Interpretability. *International Conference on Learning Representations*, 2019.
- [42] K. Yang, K. Qinami, L. Fei-Fei, J. Deng, and O. Russakovsky. Towards Fairer Datasets: Filtering and Balancing the Distribution of the People Subtree in the ImageNet Hierarchy. In *Conference on Fairness, Accountability, and Transparency*, 2020.

- [43] C. Zhang, P. Benz, T. Imtiaz, and I. S. Kweon. Understanding Adversarial Examples from the Mutual Influence of Images and Perturbations. In *Proceedings of the IEEE/CVF Conference on Computer Vision and Pattern Recognition*, pages 14521–14530, 2020.
- [44] Z. Zhao, Z. Liu, and M. Larson. On Success and Simplicity: A Second Look at Transferable Targeted Attacks. *CoRR*, abs/2012.11207, 2020.

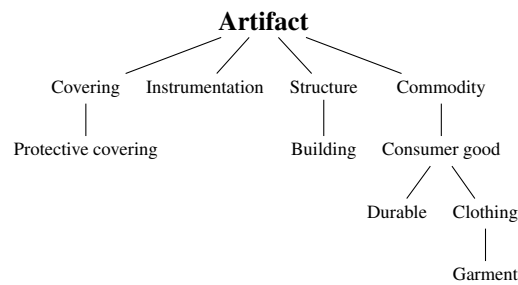
Supplementary Materials for: Evaluating Adversarial Attacks on ImageNet: A Reality Check on Misclassification Classes



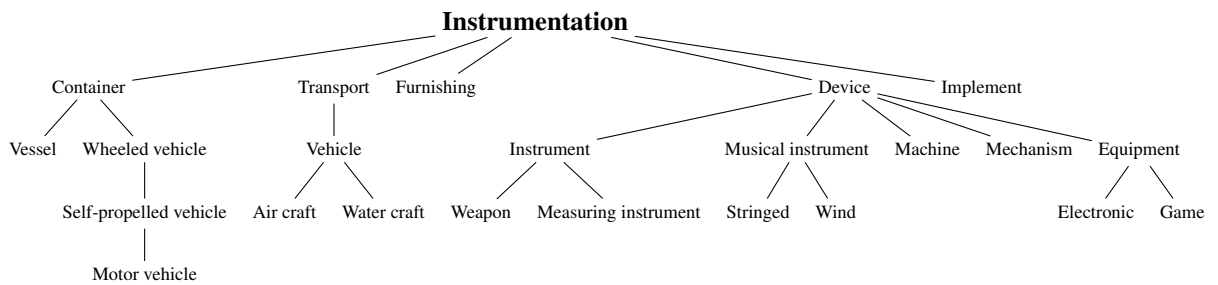
(a) Main branches of the ImageNet class hierarchy and the number of classes within those branches.



(b) ImageNet *Organism* sub-tree.



(c) ImageNet *Artifact* sub-tree.



(d) ImageNet *Instrumentation* sub-tree under *Artifact* branch.

Figure 3: The ImageNet class hierarchy: (a) main branches and the number of classes that lie in those branches, (b) view of *Organism* sub-tree, (c) view of *Artifact* sub-tree, and (d) view of *Instrumentation* sub-tree.

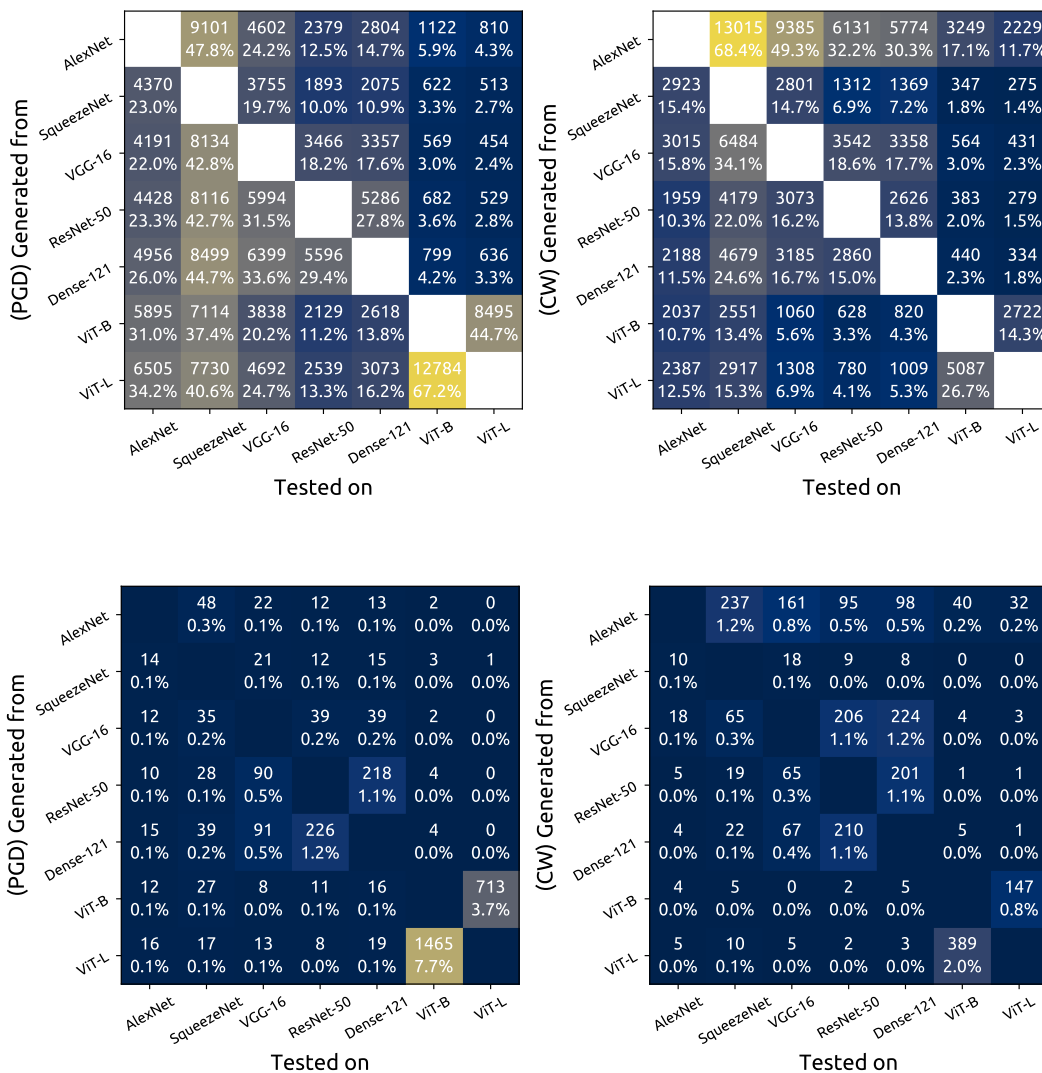


Figure 4: Number (percentage) of source images that became adversarial examples with PGD (*left*) and CW (*right*). Adversarial examples are generated by the models listed along the *y*-axis and tested by the models listed along the *x*-axis. The two figures at the top display untargeted transferability successes, whereas the two figures at the bottom display targeted transferability successes.

Table 2: For the adversarial examples that achieved model-to-model transferability and that have been created with **PGD** and **CW**, intra-collection misclassifications and misclassifications into the top- $\{3,5\}$ prediction classes in the target models are provided. The results for the adversarial examples are grouped into collections according to the classes of their source image origins.

Hierarchy	Collection	Classes in collection	Source images in collection	Adversarial examples originating from collection	Intra-collection misclassifications		Misclassification into top-K classes	
					Count	%	Top-3	Top-5
	All	1000	19,025	289,244	289,244	100.0%	59.6%	71.1%
1	Organism	410	9,390	147,621	132,865	90.0%	61.2%	72.8%
1.1	Creature	398	9,009	143,996	130,409	90.6%	61.4%	73.1%
1.1.1	Domesticated animal	123	2,316	50,036	41,978	83.9%	63.4%	75.6%
1.1.2	Vertebrate	337	7,692	126,913	112,828	88.9%	61.3%	73.2%
1.1.2.1	Mammalian	218	4,665	89,004	76,351	85.8%	61.4%	73.5%
1.1.2.1.1	Primate	20	475	9,333	5,301	56.8%	58.9%	70.4%
1.1.2.1.2	Hoofed mammal	17	419	6,206	2,751	44.3%	58.4%	71.6%
1.1.2.1.3	Feline	13	319	3,895	1,998	51.3%	64.3%	75.9%
1.1.2.1.4	Canine	130	2,502	53,294	45,089	84.6%	63.5%	75.7%
1.1.2.2	Aquatic vertebrate	16	366	5,355	2,383	44.5%	65.0%	75.6%
1.1.2.3	Bird	59	1,937	22,402	15,993	71.4%	59.8%	71.3%
1.1.2.4	Reptilian	36	547	7,635	4,795	62.8%	63.8%	75.2%
1.1.2.4.1	Saurian	11	188	2,416	1,050	43.5%	58.4%	71.1%
1.1.2.4.2	Serpent	17	223	3,202	1,700	53.1%	67.0%	77.1%
1.1.3	Invertebrate	61	1,317	17,083	10,698	62.6%	61.9%	72.3%
1.1.3.1	Arthropod	47	1,018	13,200	8,863	67.1%	63.1%	73.5%
1.1.3.1.1	Insect	27	652	7,850	4,468	56.9%	59.9%	70.5%
1.1.3.1.2	Arachnoid	9	189	2,824	1,476	52.3%	69.7%	79.5%
1.1.3.1.3	Crustacean	9	137	2,035	955	46.9%	70.0%	80.1%
2	Artifact	522	8,397	119,957	107,081	89.3%	58.6%	70.2%
2.1	Commodity	63	906	16,092	5,411	33.6%	55.5%	68.6%
2.1.1	Consumer Good	62	896	15,923	5,205	32.7%	55.5%	68.6%
2.1.1.1	Clothing	49	670	12,010	4,660	38.8%	57.5%	70.8%
2.1.1.1.1	Garment	24	295	6,218	1,455	23.4%	56.4%	70.7%
2.1.1.2	Durable	13	226	3,913	331	8.5%	49.6%	61.8%
2.2	Covering	90	1,287	20,928	9,182	43.9%	59.4%	71.9%
2.2.1	Protective covering	27	407	6,021	766	12.7%	64.6%	75.7%
2.3	Instrumentation	353	5,963	80,638	55,364	68.7%	58.0%	69.7%
2.3.1	Container	99	1,528	20,779	10,701	51.5%	62.9%	73.5%
2.3.1.1	Vessel	23	261	4,515	1,373	30.4%	57.2%	67.9%
2.3.1.2	Wheeled vehicle	43	879	9,288	5,445	58.6%	70.4%	80.0%
2.3.1.2.1	Self-propelled vehicle	31	627	6,761	3,336	49.3%	69.5%	79.7%
2.3.1.2.1.1	Motor vehicle	22	400	4,654	2,198	47.2%	67.6%	79.3%
2.3.2	Transport	71	1,558	17,929	10,643	59.4%	64.5%	75.2%
2.3.2.1	Vehicle	66	1,439	16,790	9,439	56.2%	64.3%	75.0%
2.3.2.1.1	Air craft	4	101	1,885	291	15.4%	50.7%	62.2%
2.3.2.1.2	Water craft	15	367	4,400	1,854	42.1%	59.5%	72.0%
2.3.3	Device	125	1,901	24,436	8,235	33.7%	57.5%	68.7%
2.3.3.1	Instrument	28	374	4,999	1,330	26.6%	57.6%	68.7%
2.3.3.1.1	Measuring instrument	12	202	2,605	716	27.5%	57.5%	67.4%
2.3.3.1.2	Weapon	7	69	914	150	16.4%	63.6%	72.2%
2.3.3.2	Machine	14	223	2,527	496	19.6%	69.7%	80.3%
2.3.3.3	Mechanism	12	219	2,814	45	1.6%	52.4%	63.8%
2.3.3.4	Musical instrument	26	427	4,756	1,835	38.6%	63.4%	74.1%
2.3.3.4.1	Stringed instrument	8	158	1,665	515	30.9%	61.7%	72.9%
2.3.3.4.2	Wind instrument	12	188	2,080	573	27.5%	63.3%	73.8%
2.3.4	Equipment	37	738	11,470	2,379	20.7%	50.2%	63.6%
2.3.4.1	Electronic equipment	13	178	3,122	394	12.6%	52.0%	64.9%
2.3.4.2	Game equipment	13	321	3,983	763	19.2%	56.3%	67.7%
2.3.5	Furnishing	25	447	7,554	1,774	23.5%	57.2%	69.6%
2.3.6	Implement	38	409	7,452	1,657	22.2%	57.2%	69.0%
2.4	Structure	57	1,035	12,799	5,349	41.8%	62.3%	72.1%
2.4.1	Building	14	293	3,428	663	19.3%	66.0%	76.5%
3	Geological formation	10	139	3,631	1,439	39.6%	49.4%	61.2%
3.1	Natural elevation	5	65	1,705	219	12.8%	47.6%	60.1%
4	Natural object	17	379	5,734	1,700	29.6%	52.8%	63.4%
4.1	Plant	16	363	5,207	1,700	32.6%	53.7%	63.9%
4.1.1	Fruit	16	363	5,207	1,700	32.6%	53.7%	63.9%
4.1.1.1	Edible fruit	10	233	3,564	819	23.0%	49.7%	60.5%
5	Fungus	7	226	2,307	544	23.6%	56.1%	66.4%
6	Nutrition	10	157	3,017	528	17.5%	54.8%	64.1%
7	Vegetable	13	278	4,368	1,230	28.2%	56.5%	67.7%
8	Beverage	4	40	1,226	165	13.5%	64.4%	74.3%

Table 3: For the adversarial examples that achieved model-to-model transferability and that have been created with **PGD**, intra-collection misclassifications and misclassifications into the top- $\{3,5\}$ prediction classes in the target models are provided. The results for the adversarial examples are grouped into collections according to the classes of their source image origins.

Hierarchy	Collection	Classes in collection	Source images in collection	Adversarial examples originating from collection	Intra-collection misclassifications		Misclassification into top-K classes	
					Count	%	Top-3	Top-5
	All	1000	19,025	173,549	173,549	100.0%	59.5%	71.5%
1	Organism	410	9,390	84,734	75,882	89.6%	62.0%	74.0%
1.1	Creature	398	9,009	82,599	74,498	90.2%	62.3%	74.2%
1.1.1	Domesticated animal	123	2,316	28,385	23,898	84.2%	64.6%	77.2%
1.1.2	Vertebrate	337	7,692	72,329	64,258	88.8%	62.3%	74.5%
1.1.2.1	Mammalian	218	4,665	50,125	43,705	87.2%	62.9%	75.5%
1.1.2.1.1	Primate	20	475	5,123	2,999	58.5%	60.4%	72.5%
1.1.2.1.2	Hoofed mammal	17	419	3,460	1,541	44.5%	60.2%	74.0%
1.1.2.1.3	Feline	13	319	2,346	1,262	53.8%	65.9%	78.5%
1.1.2.1.4	Canine	130	2,502	30,094	25,784	85.7%	64.8%	77.5%
1.1.2.2	Aquatic vertebrate	16	366	3,273	1,426	43.6%	64.7%	75.4%
1.1.2.3	Bird	59	1,937	12,878	9,013	70.0%	60.3%	71.4%
1.1.2.4	Reptilian	36	547	4,549	2,829	62.2%	62.7%	75.2%
1.1.2.4.1	Saurian	11	188	1,449	610	42.1%	56.5%	70.2%
1.1.2.4.2	Serpent	17	223	1,931	1,013	52.5%	66.0%	77.3%
1.1.3	Invertebrate	61	1,317	10,270	6,329	61.6%	62.0%	72.5%
1.1.3.1	Arthropod	47	1,018	7,893	5,200	65.9%	63.1%	73.7%
1.1.3.1.1	Insect	27	652	4,650	2,566	55.2%	59.7%	70.5%
1.1.3.1.2	Arachnoid	9	189	1,700	932	54.8%	70.0%	80.1%
1.1.3.1.3	Crustacean	9	137	1,247	571	45.8%	70.2%	80.5%
2	Artifact	522	8,397	75,248	67,853	90.2%	57.7%	70.0%
2.1	Commodity	63	906	10,204	3,428	33.6%	54.7%	68.5%
2.1.1	Consumer Good	62	896	10,107	3,290	32.6%	54.7%	68.4%
2.1.1.1	Clothing	49	670	7,515	2,984	39.7%	56.8%	71.0%
2.1.1.1.1	Garment	24	295	3,877	928	23.9%	55.4%	70.6%
2.1.1.1.2	Durable	13	226	2,592	187	7.2%	48.3%	60.8%
2.2	Covering	90	1,287	13,113	5,846	44.6%	58.3%	71.6%
2.2.1	Protective covering	27	407	3,793	511	13.5%	63.2%	74.7%
2.3	Instrumentation	353	5,963	50,597	34,722	68.6%	57.1%	69.4%
2.3.1	Container	99	1,528	12,966	6,622	51.1%	61.8%	72.9%
2.3.1.1	Vessel	23	261	2,789	804	28.8%	55.3%	66.0%
2.3.1.2	Wheeled vehicle	43	879	5,791	3,403	58.8%	70.1%	80.2%
2.3.1.2.1	Self-propelled vehicle	31	627	4,262	2,126	49.9%	69.4%	80.2%
2.3.1.2.1.1	Motor vehicle	22	400	2,953	1,406	47.6%	67.7%	80.1%
2.3.2	Transport	71	1,558	11,340	6,725	59.3%	63.8%	75.1%
2.3.2.1	Vehicle	66	1,439	10,604	5,946	56.1%	63.6%	74.9%
2.3.2.1.1	Air craft	4	101	1,180	193	16.4%	49.0%	61.6%
2.3.2.1.2	Water craft	15	367	2,845	1,167	41.0%	58.9%	71.7%
2.3.3	Device	125	1,901	15,419	5,212	33.8%	56.7%	68.8%
2.3.3.1	Instrument	28	374	3,088	836	27.1%	58.0%	69.3%
2.3.3.1.1	Measuring instrument	12	202	1,624	468	28.8%	57.3%	67.4%
2.3.3.1.2	Weapon	7	69	527	86	16.3%	66.6%	74.8%
2.3.3.2	Machine	14	223	1,690	293	17.3%	67.6%	79.2%
2.3.3.3	Mechanism	12	219	1,809	29	1.6%	51.1%	63.1%
2.3.3.4	Musical instrument	26	427	2,912	1,155	39.7%	62.7%	75.2%
2.3.3.4.1	Stringed instrument	8	158	1,015	324	31.9%	61.1%	74.3%
2.3.3.4.2	Wind instrument	12	188	1,283	374	29.2%	63.0%	74.8%
2.3.4	Equipment	37	738	7,257	1,555	21.4%	49.4%	64.0%
2.3.4.1	Electronic equipment	13	178	1,947	251	12.9%	49.3%	63.5%
2.3.4.2	Game equipment	13	321	2,538	510	20.1%	57.1%	69.3%
2.3.5	Furnishing	25	447	4,697	1,067	22.7%	55.5%	68.4%
2.3.6	Implement	38	409	4,544	1,013	22.3%	56.8%	69.5%
2.4	Structure	57	1,035	7,998	3,404	42.6%	62.5%	72.8%
2.4.1	Building	14	293	2,137	431	20.2%	65.2%	76.5%
3	Geological formation	10	139	2,250	860	38.2%	46.8%	59.8%
3.1	Natural elevation	5	65	1,080	123	11.4%	44.1%	58.2%
4	Natural object	17	379	3,590	1,105	30.8%	52.2%	64.3%
4.1	Plant	16	363	3,238	1,105	34.1%	53.6%	64.8%
4.1.1	Fruit	16	363	3,238	1,105	34.1%	53.6%	64.8%
4.1.1.1	Edible fruit	10	233	2,250	550	24.4%	49.0%	61.1%
5	Fungus	7	226	1,320	295	22.3%	55.4%	65.9%
6	Nutrition	10	157	1,895	340	17.9%	53.9%	63.9%
7	Vegetable	13	278	2,814	772	27.4%	56.1%	68.0%
8	Beverage	4	40	767	93	12.1%	61.4%	71.7%

Table 4: For the adversarial examples that achieved model-to-model transferability and that have been created with **CW**, intra-collection misclassifications and misclassifications into the top- $\{3,5\}$ prediction classes in the target models are provided. The results for the adversarial examples are grouped into collections according to the classes of their source image origins.

Hierarchy	Collection	Classes in collection	Source images in collection	Adversarial examples originating from collection	Intra-collection misclassifications		Misclassification into top-K classes	
					Count	%	Top-3	Top-5
	All	1000	19,025	115,695	115,695	100.0%	59.8%	70.5%
1	Organism	410	9,390	62,887	56,983	90.6%	60.1%	71.3%
1.1	Creature	398	9,009	61,397	55,911	91.1%	60.2%	71.5%
1.1.1	Domesticated animal	123	2,316	21,651	18,080	83.5%	61.8%	73.5%
1.1.2	Vertebrate	337	7,692	54,584	48,570	89.0%	60.0%	71.4%
1.1.2.1	Mammalian	218	4,665	38,879	32,646	84.0%	59.6%	71.0%
1.1.2.1.1	Primate	20	475	4,210	2,302	54.7%	57.1%	67.8%
1.1.2.1.2	Hoofed mammal	17	419	2,746	1,210	44.1%	56.2%	68.6%
1.1.2.1.3	Feline	13	319	1,549	736	47.5%	61.9%	72.0%
1.1.2.1.4	Canine	130	2,502	23,200	19,305	83.2%	61.8%	73.5%
1.1.2.2	Aquatic vertebrate	16	366	2,082	957	46.0%	65.6%	75.9%
1.1.2.3	Bird	59	1,937	9,524	6,980	73.3%	59.2%	71.1%
1.1.2.4	Reptilian	36	547	3,086	1,966	63.7%	65.4%	75.1%
1.1.2.4.1	Saurian	11	188	967	440	45.5%	61.4%	72.4%
1.1.2.4.2	Serpent	17	223	1,271	687	54.1%	68.5%	76.8%
1.1.3	Invertebrate	61	1,317	6,813	4,369	64.1%	61.8%	72.1%
1.1.3.1	Arthropod	47	1,018	5,307	3,663	69.0%	63.0%	73.3%
1.1.3.1.1	Insect	27	652	3,200	1,902	59.4%	60.2%	70.5%
1.1.3.1.2	Arachnoid	9	189	1,124	544	48.4%	69.3%	78.6%
1.1.3.1.3	Crustacean	9	137	788	384	48.7%	69.7%	79.4%
2	Artifact	522	8,397	44,709	39,228	87.7%	60.1%	70.5%
2.1	Commodity	63	906	5,888	1,983	33.7%	56.9%	68.8%
2.1.1	Consumer Good	62	896	5,816	1,915	32.9%	57.1%	68.9%
2.1.1.1	Clothing	49	670	4,495	1,676	37.3%	58.5%	70.4%
2.1.1.1.1	Garment	24	295	2,341	527	22.5%	58.1%	70.9%
2.1.1.2	Durable	13	226	1,321	144	10.9%	52.2%	63.7%
2.2	Covering	90	1,287	7,815	3,336	42.7%	61.1%	72.4%
2.2.1	Protective covering	27	407	2,228	255	11.4%	66.9%	77.4%
2.3	Instrumentation	353	5,963	30,041	20,642	68.7%	59.7%	70.1%
2.3.1	Container	99	1,528	7,813	4,079	52.2%	64.6%	74.4%
2.3.1.1	Vessel	23	261	1,726	569	33.0%	60.4%	71.0%
2.3.1.2	Wheeled vehicle	43	879	3,497	2,042	58.4%	71.1%	79.5%
2.3.1.2.1	Self-propelled vehicle	31	627	2,499	1,210	48.4%	69.8%	78.8%
2.3.1.2.1.1	Motor vehicle	22	400	1,701	792	46.6%	67.4%	78.0%
2.3.2	Transport	71	1,558	6,589	3,918	59.5%	65.7%	75.4%
2.3.2.1	Vehicle	66	1,439	6,186	3,493	56.5%	65.5%	75.2%
2.3.2.1.1	Air craft	4	101	705	98	13.9%	53.5%	63.1%
2.3.2.1.2	Water craft	15	367	1,555	687	44.2%	60.6%	72.7%
2.3.3	Device	125	1,901	9,017	3,023	33.5%	58.9%	68.6%
2.3.3.1	Instrument	28	374	1,911	494	25.9%	56.9%	67.8%
2.3.3.1.1	Measuring instrument	12	202	981	248	25.3%	57.8%	67.4%
2.3.3.1.2	Weapon	7	69	387	64	16.5%	59.4%	68.7%
2.3.3.2	Machine	14	223	837	203	24.3%	74.0%	82.6%
2.3.3.3	Mechanism	12	219	1,005	16	1.6%	54.7%	65.1%
2.3.3.4	Musical instrument	26	427	1,844	680	36.9%	64.5%	72.4%
2.3.3.4.1	Stringed instrument	8	158	650	191	29.4%	62.8%	70.8%
2.3.3.4.2	Wind instrument	12	188	797	199	25.0%	63.7%	72.3%
2.3.4	Equipment	37	738	4,213	824	19.6%	51.7%	62.8%
2.3.4.1	Electronic equipment	13	178	1,175	143	12.2%	56.4%	67.2%
2.3.4.2	Game equipment	13	321	1,445	253	17.5%	54.9%	64.8%
2.3.5	Furnishing	25	447	2,857	707	24.7%	60.0%	71.6%
2.3.6	Implement	38	409	2,908	644	22.1%	57.9%	68.3%
2.4	Structure	57	1,035	4,801	1,945	40.5%	62.2%	71.0%
2.4.1	Building	14	293	1,291	232	18.0%	67.4%	76.4%
3	Geological formation	10	139	1,381	579	41.9%	53.8%	63.4%
3.1	Natural elevation	5	65	625	96	15.4%	53.8%	63.2%
4	Natural object	17	379	2,144	595	27.8%	53.7%	61.9%
4.1	Plant	16	363	1,969	595	30.2%	53.9%	62.3%
4.1.1	Fruit	16	363	1,969	595	30.2%	53.9%	62.3%
4.1.1.1	Edible fruit	10	233	1,314	269	20.5%	50.9%	59.5%
5	Fungus	7	226	987	249	25.2%	57.1%	67.2%
6	Nutrition	10	157	1,122	188	16.8%	56.3%	64.4%
7	Vegetable	13	278	1,554	458	29.5%	57.3%	67.3%
8	Beverage	4	40	459	72	15.7%	69.5%	78.6%

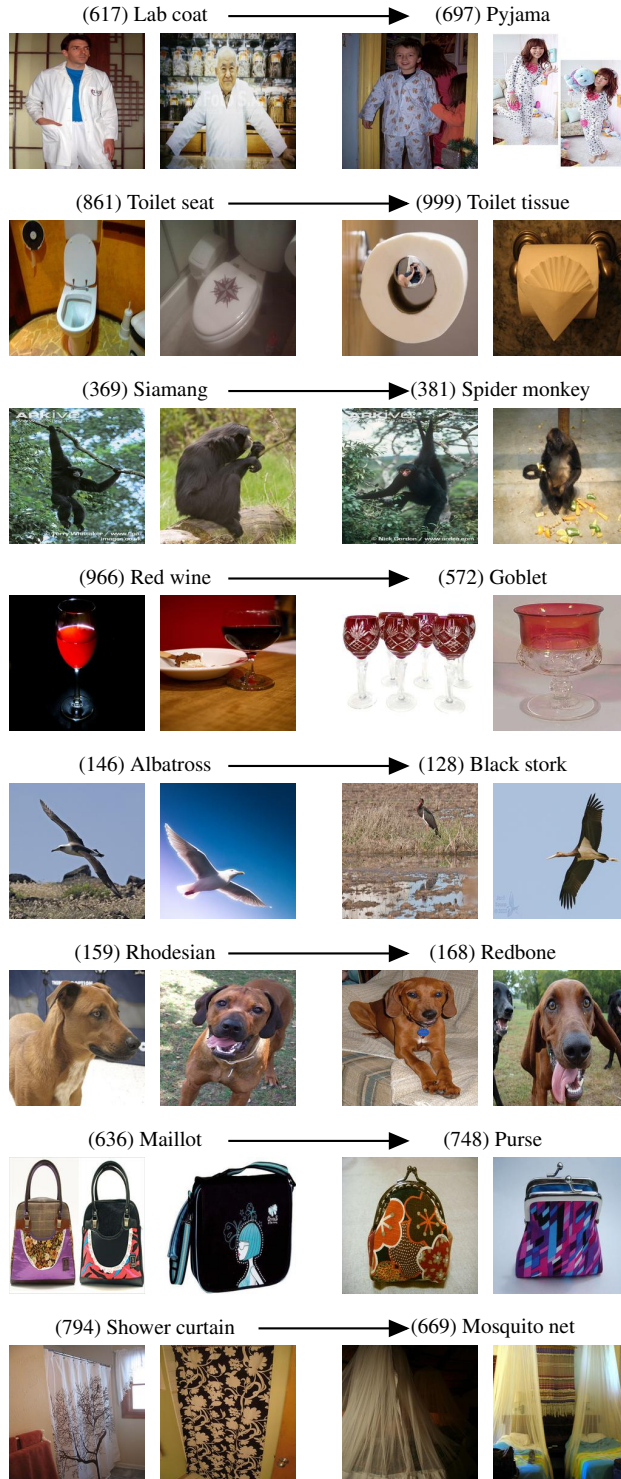


Figure 5: Adversarial examples on the left are misclassified into the classes on the right by multiple models used in this study. The classes given on the right often lie in the top-5 predictions for the genuine source image counterparts of those adversarial examples.

Table 5: For the adversarial examples that achieved model-to-model transferability and that have been created with **PGD** and **CW**, intra-collection misclassifications and misclassifications into the top- $\{3,5\}$ prediction classes in the target models are provided for each model employed in this study (1st column). The results for the adversarial examples are grouped into collections according to the classes of their source image origins. The results are provided for a number of collections that lie under the **Organism** sub-tree.

Model	Hierarchy	Collection	Classes in collection	Source images in collection	Adversarial examples originating from collection	Intra-collection misclassifications		Misclassification into top-K classes	
						Count	%	Top-3	Top-5
AlexNet	1	Organism	410	9,390	23,841	21,977	92.2%	76.0%	86.8%
	1.1.2.1.1	Primate	20	475	1,587	755	47.6%	78.3%	88.6%
	1.1.2.1.2	Hoofed mammal	17	419	1,044	420	40.2%	70.1%	86.9%
	1.1.2.1.3	Feline	13	319	781	354	45.3%	74.6%	89.2%
	1.1.2.1.4	Canine	130	2,502	8,709	7,112	81.7%	77.2%	87.7%
	1.1.2.2	Aquatic vertebrate	16	366	721	313	43.4%	84.6%	92.8%
	1.1.2.3	Bird	59	1,937	3,841	2,732	71.1%	74.2%	85.1%
	1.1.2.4	Reptilian	36	547	1,415	832	58.8%	73.5%	86.1%
	1.1.3	Invertebrate	61	1,317	2,620	1,740	66.4%	75.6%	84.9%
SqueezeNet	1	Organism	410	9,390	41,266	36,530	88.5%	62.5%	75.4%
	1.1.2.1.1	Primate	20	475	2,589	1,235	47.7%	61.7%	73.7%
	1.1.2.1.2	Hoofed mammal	17	419	1,909	699	36.6%	60.9%	74.5%
	1.1.2.1.3	Feline	13	319	1,267	563	44.4%	62.7%	76.0%
	1.1.2.1.4	Canine	130	2,502	13,931	11,172	80.2%	63.2%	76.5%
	1.1.2.2	Aquatic vertebrate	16	366	1,459	530	36.3%	66.0%	77.9%
	1.1.2.3	Bird	59	1,937	6,850	4,476	65.3%	61.3%	73.6%
	1.1.2.4	Reptilian	36	547	2,349	1,348	57.4%	65.7%	78.2%
	1.1.3	Invertebrate	61	1,317	4,900	2,615	53.4%	62.1%	74.8%
VGG-16	1	Organism	410	9,390	25,580	23,658	92.5%	56.1%	68.7%
	1.1.2.1.1	Primate	20	475	1,589	1,051	66.1%	52.5%	63.6%
	1.1.2.1.2	Hoofed mammal	17	419	999	511	51.2%	53.6%	66.6%
	1.1.2.1.3	Feline	13	319	570	332	58.2%	62.3%	73.3%
	1.1.2.1.4	Canine	130	2,502	9,241	7,901	85.5%	58.3%	71.3%
	1.1.2.2	Aquatic vertebrate	16	366	1,017	472	46.4%	59.1%	70.9%
	1.1.2.3	Bird	59	1,937	4,085	3,200	78.3%	55.0%	68.6%
	1.1.2.4	Reptilian	36	547	1,096	784	71.5%	62.0%	75.8%
	1.1.3	Invertebrate	61	1,317	2,969	1,933	65.1%	57.5%	67.7%
DenseNet-121	1	Organism	410	9,390	16,477	15,181	92.1%	64.3%	75.3%
	1.1.2.1.1	Primate	20	475	1,019	697	68.4%	61.7%	73.7%
	1.1.2.1.2	Hoofed mammal	17	419	650	335	51.5%	59.5%	72.2%
	1.1.2.1.3	Feline	13	319	248	161	64.9%	73.0%	79.0%
	1.1.2.1.4	Canine	130	2,502	6,150	5,596	91.0%	67.6%	79.9%
	1.1.2.2	Aquatic vertebrate	16	366	671	363	54.1%	67.1%	76.5%
	1.1.2.3	Bird	59	1,937	2,260	1,731	76.6%	65.7%	75.6%
	1.1.2.4	Reptilian	36	547	844	551	65.3%	61.5%	70.5%
	1.1.3	Invertebrate	61	1,317	1,963	1,343	68.4%	63.3%	72.6%
ResNet-50	1	Organism	410	9,390	17,487	15,948	91.2%	59.6%	70.8%
	1.1.2.1.1	Primate	20	475	1,232	695	56.4%	50.0%	62.9%
	1.1.2.1.2	Hoofed mammal	17	419	790	407	51.5%	54.3%	67.8%
	1.1.2.1.3	Feline	13	319	318	217	68.2%	70.8%	76.7%
	1.1.2.1.4	Canine	130	2,502	6,346	5,566	87.7%	62.4%	74.2%
	1.1.2.2	Aquatic vertebrate	16	366	694	316	45.5%	60.5%	70.2%
	1.1.2.3	Bird	59	1,937	2,568	2,140	83.3%	64.3%	74.4%
	1.1.2.4	Reptilian	36	547	749	520	69.4%	63.4%	73.2%
	1.1.3	Invertebrate	61	1,317	1,792	1,284	71.7%	61.6%	73.0%
Vit-Base	1	Organism	410	9,390	13,952	11,835	84.8%	45.6%	55.6%
	1.1.2.1.1	Primate	20	475	824	498	60.4%	37.3%	49.3%
	1.1.2.1.2	Hoofed mammal	17	419	490	224	45.7%	42.0%	50.6%
	1.1.2.1.3	Feline	13	319	409	209	51.1%	50.6%	61.9%
	1.1.2.1.4	Canine	130	2,502	5,308	4,550	85.7%	52.5%	64.0%
	1.1.2.2	Aquatic vertebrate	16	366	477	234	49.1%	49.5%	61.8%
	1.1.2.3	Bird	59	1,937	1,821	1,093	60.0%	31.6%	41.1%
	1.1.2.4	Reptilian	36	547	754	475	63.0%	51.9%	59.2%
	1.1.3	Invertebrate	61	1,317	1,685	1,023	60.7%	48.5%	57.6%
Vit-Large	1	Organism	410	9,390	9,018	7,736	85.8%	52.4%	62.0%
	1.1.2.1.1	Primate	20	475	493	370	75.1%	55.2%	63.5%
	1.1.2.1.2	Hoofed mammal	17	419	324	155	47.8%	53.4%	59.9%
	1.1.2.1.3	Feline	13	319	302	162	53.6%	53.0%	61.3%
	1.1.2.1.4	Canine	130	2,502	3,609	3,192	88.4%	56.2%	68.3%
	1.1.2.2	Aquatic vertebrate	16	366	316	155	49.1%	63.9%	71.5%
	1.1.2.3	Bird	59	1,937	977	621	63.6%	40.9%	49.4%
	1.1.2.4	Reptilian	36	547	428	285	66.6%	52.1%	61.7%
	1.1.3	Invertebrate	61	1,317	1,154	760	65.9%	59.2%	65.3%

Table 6: For the adversarial examples that achieved model-to-model transferability and that have been created with **PGD** and **CW**, intra-collection misclassifications and misclassifications into the top- $\{3,5\}$ prediction classes in the target models are provided for each model employed in this study (1st column). The results for the adversarial examples are grouped into collections according to the classes of their source image origins. The results are provided for a number of collections that lie under the **Artifact** sub-tree.

Model	Hierarchy	Collection	Classes in collection	Source images in collection	Adversarial examples originating from collection	Intra-collection misclassifications		Misclassification into top-K classes	
						Count	%	Top-3	Top-5
AlexNet	2	Artifact	522	8,397	18,149	16,341	90.0%	72.5%	83.8%
	2.1.1.1	Clothing	49	670	1,790	833	46.5%	67.0%	80.2%
	2.2	Covering	90	1,287	2,960	1,386	46.8%	68.4%	81.2%
	2.3.1	Container	99	1,528	3,396	1,806	53.2%	79.3%	86.8%
	2.3.1.2	Wheeled vehicle	43	879	1,554	927	59.7%	84.6%	92.9%
	2.3.3	Device	125	1,901	4,099	1,385	33.8%	71.8%	83.8%
	2.3.3.4	Musical instrument	26	427	915	402	43.9%	74.4%	86.0%
	2.3.4	Equipment	37	738	1,778	355	20.0%	63.7%	79.6%
	2.4	Structure	57	1,035	1,733	876	50.5%	84.2%	91.6%
SqueezeNet	2	Artifact	522	8,397	35,748	32,165	90.0%	58.7%	71.0%
	2.1.1.1	Clothing	49	670	3,474	1,038	29.9%	58.8%	72.4%
	2.2	Covering	90	1,287	5,963	2,240	37.6%	60.8%	73.6%
	2.3.1	Container	99	1,528	6,041	3,061	50.7%	60.4%	72.9%
	2.3.1.2	Wheeled vehicle	43	879	2,958	1,646	55.6%	66.5%	78.0%
	2.3.3	Device	125	1,901	7,781	2,282	29.3%	57.7%	70.5%
	2.3.3.4	Musical instrument	26	427	1,674	428	25.6%	62.5%	75.0%
	2.3.4	Equipment	37	738	3,732	588	15.8%	47.4%	60.9%
	2.4	Structure	57	1,035	3,344	1,573	47.0%	65.5%	76.6%
VGG-16	2	Artifact	522	8,397	20,329	18,204	89.5%	52.9%	66.0%
	2.1.1.1	Clothing	49	670	2,197	929	42.3%	50.2%	64.7%
	2.2	Covering	90	1,287	3,729	1,822	48.9%	53.5%	67.4%
	2.3.1	Container	99	1,528	3,272	1,758	53.7%	55.8%	69.8%
	2.3.1.2	Wheeled vehicle	43	879	1,221	784	64.2%	69.5%	81.7%
	2.3.3	Device	125	1,901	4,082	1,334	32.7%	51.4%	62.5%
	2.3.3.4	Musical instrument	26	427	697	265	38.0%	55.4%	65.6%
	2.3.4	Equipment	37	738	2,132	451	21.2%	47.0%	60.0%
	2.4	Structure	57	1,035	1,833	759	41.4%	56.9%	68.4%
DenseNet-121	2	Artifact	522	8,397	14,699	12,978	88.3%	60.5%	71.5%
	2.1.1.1	Clothing	49	670	1,487	593	39.9%	56.6%	70.5%
	2.2	Covering	90	1,287	2,699	1,239	45.9%	61.1%	73.1%
	2.3.1	Container	99	1,528	2,566	1,317	51.3%	69.9%	76.9%
	2.3.1.2	Wheeled vehicle	43	879	1,122	678	60.4%	76.9%	82.1%
	2.3.3	Device	125	1,901	2,963	1,163	39.3%	61.5%	72.3%
	2.3.3.4	Musical instrument	26	427	577	310	53.7%	69.0%	78.5%
	2.3.4	Equipment	37	738	1,246	346	27.8%	50.0%	63.0%
	2.4	Structure	57	1,035	1,700	639	37.6%	63.5%	72.4%
ResNet-50	2	Artifact	522	8,397	12,887	11,576	89.8%	57.7%	69.2%
	2.1.1.1	Clothing	49	670	1,352	528	39.1%	63.1%	75.3%
	2.2	Covering	90	1,287	2,376	1,112	46.8%	64.7%	76.4%
	2.3.1	Container	99	1,528	2,210	1,156	52.3%	62.3%	73.1%
	2.3.1.2	Wheeled vehicle	43	879	911	589	64.7%	73.4%	82.8%
	2.3.3	Device	125	1,901	2,285	832	36.4%	55.7%	65.9%
	2.3.3.4	Musical instrument	26	427	341	180	52.8%	64.5%	73.6%
	2.3.4	Equipment	37	738	1,181	242	20.5%	48.9%	62.1%
	2.4	Structure	57	1,035	1,501	561	37.4%	57.5%	68.9%
Vit-Base	2	Artifact	522	8,397	10,771	9,359	86.9%	47.1%	56.2%
	2.1.1.1	Clothing	49	670	1,042	454	43.6%	48.9%	60.5%
	2.2	Covering	90	1,287	1,918	837	43.6%	48.1%	59.3%
	2.3.1	Container	99	1,528	1,893	923	48.8%	49.3%	58.4%
	2.3.1.2	Wheeled vehicle	43	879	906	490	54.1%	54.3%	62.4%
	2.3.3	Device	125	1,901	1,998	738	36.9%	40.8%	48.7%
	2.3.3.4	Musical instrument	26	427	341	135	39.6%	46.3%	53.4%
	2.3.4	Equipment	37	738	892	247	27.7%	44.1%	54.8%
	2.4	Structure	57	1,035	1,488	539	36.2%	45.9%	53.6%
Vit-Large	2	Artifact	522	8,397	7,374	6,458	87.6%	54.3%	63.2%
	2.1.1.1	Clothing	49	670	668	285	42.7%	53.0%	64.7%
	2.2	Covering	90	1,287	1,283	546	42.6%	52.5%	63.0%
	2.3.1	Container	99	1,528	1,401	680	48.5%	56.7%	66.6%
	2.3.1.2	Wheeled vehicle	43	879	616	331	53.7%	63.1%	71.1%
	2.3.3	Device	125	1,901	1,228	501	40.8%	49.5%	57.3%
	2.3.3.4	Musical instrument	26	427	211	115	54.5%	59.7%	66.8%
	2.3.4	Equipment	37	738	509	150	29.5%	52.1%	62.7%
	2.4	Structure	57	1,035	1,200	402	33.5%	55.1%	63.6%